Railyard Worker Safety through innovative Mobile Active Train Detection and Risk Localization

Hamid Sharif, Ph. D.
Charles Vranek Professor
Electrical and Computer Engineering Department
University of Nebraska-Lincoln

Michael Hempel, Ph. D.
Research Assistant Professor
Electrical and Computer Engineering Department
University of Nebraska-Lincoln

A Report on Research Sponsored by

University Transportation Center for Railway Safety (UTCRS)

University of Nebraska-Lincoln

August 2018

TECHNICAL REPORT DOCUMENTATION PAGE

1. Report No. 26-1121-0018-006	**2. Government Accession No.**	**3. Recipient's Catalog No.**
4. Title and Subtitle Railyard Worker Safety through innovative Mobile Active Train Detection and Risk Localization		**5. Report Date** August 2018 **6. Performing Organization Code**
7. Author(s) Hamid Sharif, Ph.D. Michael Hempel, Ph.D.		**8. Performing Organization Report No.** 26-1121-0018-006
9. Performing Organization Name and Address Nebraska Transportation Center University of Nebraska-Lincoln Prem S. Paul Research Center at Whittier School 2200 Vine Street Lincoln, NE 68583-0853		**10. Work Unit No.** **11. Contract or Grant No.** DTRT13-G-UTC59
12. Sponsoring Agency Name and Address University Transportation Center for Railway Safety The University of Texas Rio Grande Valley 1201 W University Drive Edinburg, Texas 78539		**13. Type of Report and Period Covered** Final Report (July 2016 – June 2018) **14. Sponsoring Agency Code**
15. Supplementary Notes Conducted in cooperation with the U.S. Department of Transportation, Federal Highway Administration.		

16. Abstract

This project aimed at improving the safety of railyard workers by increasing overall situational awareness. To accomplish this we research sensing technologies that can be used to detect objects, classify them, and localize them. Once localized, proximity of dangerous objects to railyard workers can be detected and alerts can be triggered. This project explored the use of vision-based systems as well as Software-Defined RADAR, in combination with each other, to provide observations reliably under a wide range of weather conditions. We conducted a large number of field tests using Software Defined RADAR at the Union Pacific Yard which the results have shown the tremendous potential in this approach. We also developed several signal processing approaches as part of the project effort. We look forward to further exploring this application, as well as other related applications for this technology. We would like to thank Union Pacific for all their assistance with this project.

17. Key Words Railroad, Railyard, Safety, Wearable, Sensing, RADAR	**18. Distribution Statement** No restrictions.		
19. Security Classif. (of this report) unclassified	**20. Security Classif. (of this page)** unclassified	**21. No. of Pages** 43	**22. Price**

Form DOT F 1700.7 (8-72) Reproduction of completed page authorized

Table of Contents

Abstract vii
Chapter 1 Introduction 1
Chapter 2 Overall Approach 2
2.1 Study of Different Sensor Types 3
2.2 Camera-Based Approach 4
2.3 RADAR-Based Approach 5
Chapter 3 Field Tests 20
3.1 Field Test: Settings and their Descriptions in gSDR 20
3.2 Field Tests at Union Pacific Railyard 23
3.2.1 Field Test List & Brief Summary 23
Chapter 4 Summary and Conclusions 40
4.1 Summary 40
4.2 Publications Resulting from Research 40
4.3 Conclusions and Future Work 41
References 43

List of Figures

Figure 2.1 Vision-based Vehicle detection: a) raw sensor image, b) unrolled image, c) edge detection, d) region-of-interest detection, e) car classification and range estimation 5
Figure 2.2 The SDRadar with its antenna setup (left), and the main system board (right) 6
Figure 2.3 FMCW in time and frequency.....7
Figure 2.4 Our gSDR viewer (i), a scenario with a car approaching and a pedestrian walking away from the radar (ii), a scenario with multiple pedestrians walking at different speeds 8
Figure 2.5 3D plot of a RADAR return waterfall plot showing the same data set as in Fig 2.4-ii..9
Figure 2.6 Parking Lot test setup with RADAR facing down straight parking lot section 10
Figure 2.7 RADAR Reflector test used in pedestrian test scenarios 10
Figure 2.8 Slight side-view of the Rails West/Council Bluffs site radar configuration, showing radar placement, and main train path.....12
Figure 2.9 Rails West/Council Bluffs Field Test Configuration (Top View). The red shaded area shows the main area of focus. The Iowa Interstate Railroad Council Bluffs Yard is South-East of the above traffic intersection along the Train Path indicated in the above figure 14
Figure 2.10 Ancortek's SDR 580B-Kit used in all tests conducted 15
Figure 2.11 gSDR software, custom-written software by UNL's TEL group, running in MATLAB.....16
Figure 2.12 (left) Radar setup with laptop, tripod and video camera. (right) Closeup of radar transmit and receive antenna and control unit (blue box).....17
Figure 2.13 Another view of the passing train.....18
Figure 2.14 Radar Field testing setup while a locomotive passes by 19
Figure 3.1 Field Test configuration for Test 00 25
Figure 3.2 Waterfall plot of Power Spectral Density (PSD) for Test00 26
Figure 3.3 Waterfall plot of Power Spectral Density (PSD) for Test01 27
Figure 3.4 Field Test Configuration for Test02 29
Figure 3.5 Waterfall plot of Power Spectral Density (PSD) for Test02. Notice return is initially strong, but then generally softer.....30
Figure 3.6 Initial set of locomotives, with sharp edges and rectangular nature provides a larger RCS to the radar.....31
Figure 3.7 The remaining locomotives were more cylindrical causing the radar signals to spread out and yielding a 'softer' return.....31
Figure 3.8 Field Test Configuration for Test03. Note the 'Train Path' is actually opposite of what is shown above.....32
Figure 3.9 Waterfall plot of Power Spectral Density (PSD) for Test03as it entered the radar's FOV 33
Figure 3.10 Waterfall plot of Power Spectral Density (PSD) for Test03 34
Figure 3.11 Field Test Configuration for Test04 35
Figure 3.12 Waterfall plot of Power Spectral Density (PSD) for Test04 36
Figure 3.13 Power Spectral Density (PSD) of a single 'slice' of the waterfall plot for Test02.....37
Figure 3.14 Signal Processing Phases in our SDROT tool (Software Defined RADAR Object Tracking).....38
Figure 3.15 Object Tracking over Time 39

List of Tables

Table 2.1 Comparison of proximity detection technologies.....3

Disclaimer

The contents of this report reflect the views of the authors, who are responsible for the facts and the accuracy of the information presented herein. This document is disseminated in the interest of information exchange. The report is funded, partially or entirely, by a grant from the U.S. Department of Transportation's University Transportation Centers Program. However, the U.S. Government assumes no liability for the contents or use thereof.

Abstract

This project aimed at improving the safety of railyard workers by increasing overall situational awareness. To accomplish this, we research sensing technologies that can be used to detect objects, classify them, and localize them. Once localized, proximity of dangerous objects to railyard workers can be detected and alerts can be triggered. This project explored the use of vision-based systems as well as Software-Defined RADAR, in combination with each other, to provide observations reliably under a wide range of weather conditions. We conducted a large number of field tests using Software Defined RADAR at the Union Pacific Yard, which the results have shown the tremendous potential in this approach. We also developed several signal processing approaches as part of the project effort. We look forward to further exploring this application, as well as other related applications for this technology. We would like to thank Union Pacific for all their assistance with this project.

Chapter 1 Introduction

The railroad industry in North America continues its efforts to improve the safety of their personnel. This includes railyard worker safety, who work in an environment where it is often infeasible to detect approaching threats such as railyard vehicles, locomotives, or railcars, while focusing on their specific tasks. This risk is elevated through the use of Remote Control Locomotives (RCL), where there is oftentimes no engineer in the locomotive, but that are rather operated via remote control console from the rear of a train. Enhancing railyard worker safety through technology that is wearable, reliable, and accurate, is a stated interest of the railroads. We therefore focused our efforts throughout this project on researching an easy-to-deploy, effective, and robust solution for automated threat detection, localization, and alerting.
For this solution we proposed to study a variety of different detection approaches, such as passive acoustic localization using microphone arrays for precise distance and direction determination, 360degree point-of-view (POV) camera systems and active image processing to visually detect trains, active echo localization for moving obstacle detection, and RF & EM detection to detect interference from the locomotive itself. The overall architecture includes sensor data processing research to extract insights from the raw sensor data, as well as possibly classify threats, and sharing of these results wirelessly with railyard workers and a central data collection site for.

We believe that the insights from this project represent a vital cornerstone in the efforts to further enhance railyard worker safety and prevent accidents and the potential loss of life.

Chapter 2 Overall Approach

Our first priority was to collect insights from the railroad industry on their own past efforts, possible requirements, and constraints. We had seven discussions with different groups at the Union Pacific Railroad to understand these priorities.

Summarizing the key takeaways from this collaboration resulted in the following guidelines:

- The system could not impede the movement of the railyard workers. This was paramount.
- The system could also not cause any significant increase in the workload of railyard workers, or otherwise be a significant burden to them.
- The system needs to be able to perform in a wide variety of yard, under a wide variety of weather conditions.

These three tenets guided the entire project. Our next step involved a review of existing sensing technologies, to generally explore their feasibility for use in the envisioned architecture. That architecture involved, abstractly, a self-contained system with one or more sensor, processing capabilities, and wireless communication capabilities.

Once we had evaluated various different sensors we proceeded with exploring them specifically for detection and localization of humans and rail vehicles, being able to localize them, and finally being able to distinguish between them. We also explored the use of wearables as personal worker health monitoring devices, such as for the detection of trips and falls, aberrant heartrate, or dehydration. In combination, our worker locators and the personal wearables would provide all the required capabilities we set out to achieve.

Table 2.1 Comparison of proximity detection technologies

Criteria	Technologies													
	Ultrasound	**ultra-high frequency (UHF)**	**Very High Frequency (VHF)**	**image stream**	**eye-safe laser**	**RADAR (mmWave, VHF/UHF, microwave, etc.)**	**Infrared**	**LIDAR**	**Vibration/ Acoustic Sensor**	**Magnetic Sensor**	**UWB/mmWave**	**Chirp Spread Spectrum**	**GPS**	**RFID**
Range [m]	0-15	0-40	0-500	0-500	0-50	0-100	0-30	0-100	0-100	0-100	0-150	0-1000	n/a	0-100
Accuracy	Low	medium	medium	medium	High	High	low	high	low	low	medium/high	medium/high	High	medium
Rebound signal	High	small	medium/high	high		High	high	high	high		low/medium	high	Low	high
Computational complexity	Low	low	low	high/medium	high/medium	small/high	low	small/high	low/medium	low	low/medium	low	low	low
signal robustness	noisy	yes	yes	no	No	Yes	no	yes	no	no	yes	medium/high	medium	low
low visibility	very good	very good	very good	poor	very good	very good	good	very good	good	good	very good	high	high	high
update rate	high	high	high	high	High	High		high	high	high	high	high	high	high
size & weight	small	small	small	small	Medium	large/medium	small	medium/large	small/medium	small	small	low	low	low
Installation/maintenance	small	small	small	small/medium	small/medium	high/medium	small	high/medium	small/medium	small	small/medium	low	low	low
power consumption	small	small	small/medium	high/medium	high/medium	High	small	high	small/medium	small	small/medium	low	low	low
disadvantage	short range/noisy	proximity	Omni directional signal/proximity	power consumption/ computational complexity/LOS/ poor performance in low visibility	power consumption /LOS	power consumption/ bulky	LOS/ noisy	bulky/power consumption	proximity, computation complexity	proximity, interference	multipath propagation	interference	accuracy	accuracy
wearable	yes	yes	yes	**	**	No	yes	no	yes	no*	yes	yes	yes	yes
benefits	low cost	performs in metallic region	long range	long range/location	long range/location tracking	long range/ location tracking	low cost	range/ location tracking	low cost	low cost	location/ range	low cost/accurate	low cost	low power consumption
ideal operational area	construction/emergency	construction/ railroads	railroads	railroads, construction	construction, emergency	construction, railroads, emergency	construction	emergency, construction	railroads	construction, railroad	construction, railroad, emergency	railroad, construction	rail road	rail road, construction
cost	low	low	low	medium	medium/high	High	low	high	low	low	high	low	low	high
Field of View	medium	high	medium	low/medium	Low	High	low	high	high	high	high	high	high	high
Best use	proximity	proximity/location tracking	location tracking		proximity/distance/3D-4D point cloud		proximity	proximity/3D cloud	proximity	proximity, interference	location tracking/proximity	location tracking	location tracking	location tracking
Deployment	at hump, or near track, over workers, equipment	antennas all over the region (triangulation)	antennas all over the region (triangulation) + over	at hump (placed high above ground) + wearable	at hump (placed above ground)	at hump	as sensor network	at hump (placed above ground)	placed over track or hump	placed above track	Placed strategically	placed strategically	placed over assets and workers	placed over assets and workers

2.1 Study of Different Sensor Types

But key to the success of this project was the ability to detect and localize individual workers and vehicles. As shown earlier, this could not impede the workers or cause extra workloads, and it needed to work in adverse environmental conditions.

The types of sensors we investigated, as well as our findings, we published in [1]. Table 2.1 summarizes those findings [1]. What we found is that the two most promising technologies were vision-based systems, as well as RADAR/LIDAR. Vision-based system provide range, and the scientific community has developed a vast set of image processing techniques to detect, classify, and localize objects of interest. But vision-based systems do not work well under adverse weather conditions, such as rain, snow, or fog. They also do not work well in low-light

conditions. Therefore, our solution is to augment such a system with a RADAR or LIDAR system. These systems work significantly better under adverse weather conditions than vision-based systems, and would therefore well-complement our solution.

2.2 Camera-Based Approach

For our tests we developed a light-weight and wearable fisheye camera system that acquired images and provided them to an image-processing system. There, we unrolled the fisheye distortions and then conducted object detection. Once we detected regions within the imagery that contained objects of interest we classified them. Once we knew what they were, we could use a reference catalog to estimate the real-world size of these objects based on their image-based dimensions. This process is shown in the following image set:

(a)

(b)

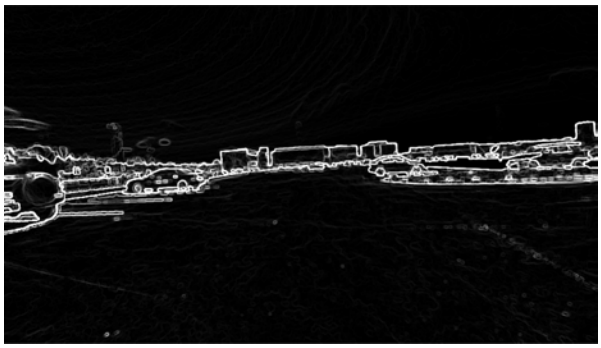

(c)

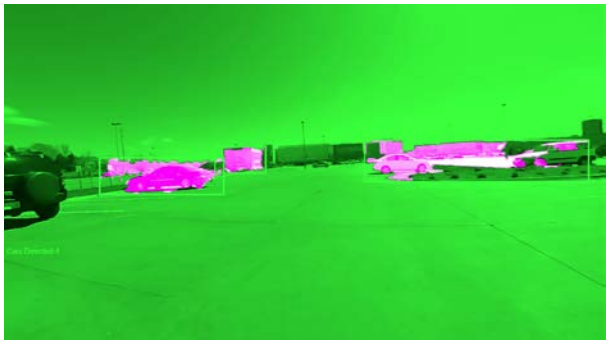

(d)

(e)

Figure 2.1 Vision-based Vehicle detection: a) raw sensor image, b) unrolled image, c) edge detection, d) region-of-interest detection, e) car classification and range estimation

2.3 RADAR-Based Approach

Once we validated that vision-based systems could be successfully employed to detect, classify, and range objects of interest, we next focused on RADAR-based systems. In particular, we decided to leverage a recent technological advance called Software-Defined RADAR. This

combines the work done for software-defined radios in wireless communications and adapts it to the use for ranging applications. The advantage of this technology is that, similar to software radios, the parameters with which the RADAR is operated are fully controlled by software, down to the generated signal. Hence, we can adapt the detection signal to achieve the desired range or resolution. For example, detecting faraway objects requires us to adjust for increased maximum detection range, but that also reduces the object resolution and thus makes it more difficult to distinguish humans from vehicles at those distances. But when all objects are close to the RADAR, we can adapt the RADAR to reduce its distance in favor of resolution, to make it easier to classify the observed objects. Over time, we can thus track objects through the RADAR's observable range and always adapt to optimal parameter sets. This is key to keeping the RADAR small-scale yet effective.

For our tests we decided to utilize Ancortek's 5.8GHz SDRadar kit, because it allows us to operate a RADAR in a license-free frequency band, achieve high resolution and relatively high range for a transmit-power limited RADAR system. Below are two images that show the device and overall setup with its dual antennas:

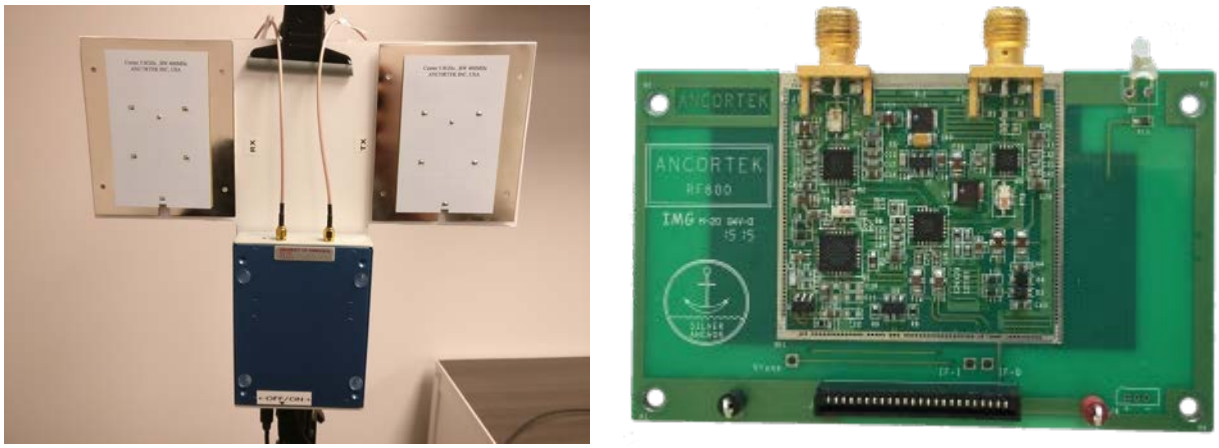

Figure 2.2 The SDRadar with its antenna setup (left), and the main system board (right)

The preferred waveform in most of our tests was a frequency modulated continuous wave (FMCW) waveform. The image below shows a representation of an FMCW waveform in time and frequency. We can clearly see the applied banding in FMCW and the rotation over time of which band is assigned maximum power.

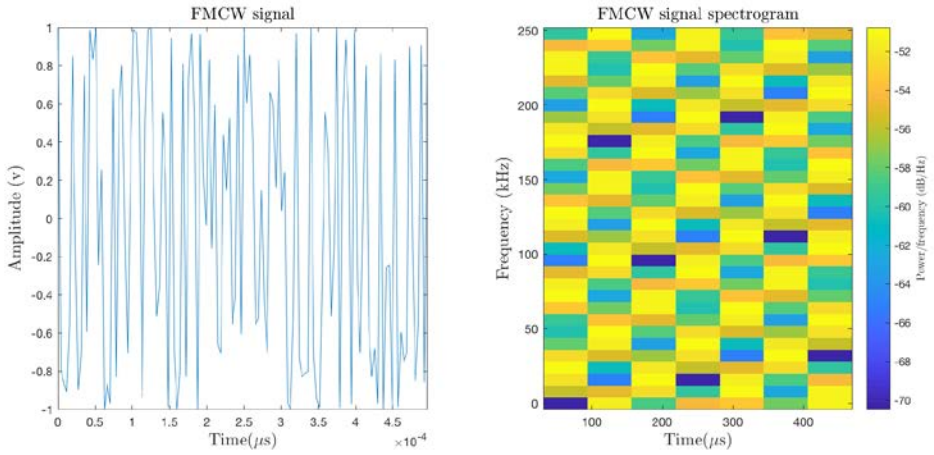

Figure 2.3 FMCW in time and frequency.

For our tests with the Ancortek SDRADAR kit we also developed our own signal acquisition and processing solution. This application and two sample recordings are shown in the following figure.

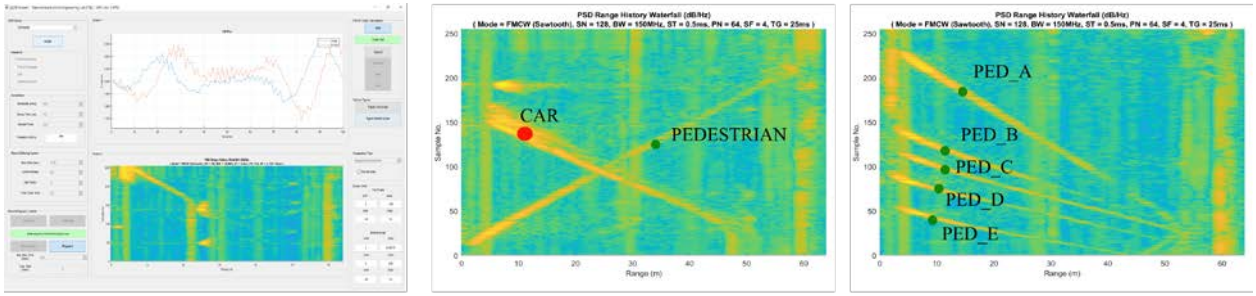

(i) (ii) (iii)

Figure 2.4 Our gSDR viewer (i), a scenario with a car approaching and a pedestrian walking away from the radar (ii), a scenario with multiple pedestrians walking at different speeds

The tests shown in figure 2.4 were conducted in our parking lot. They clearly show the ability of identifying different objects and being able to track them over time. They also show that it is possible to distinguish between cars and pedestrians. We developed processing algorithms that perform all of these tasks autonomously on the recording data, from filtering, velocity extraction, to object tracking. We also begun efforts as part of this seed study to classify detected objects. The images below show some of the figures obtained from the preliminary tests:

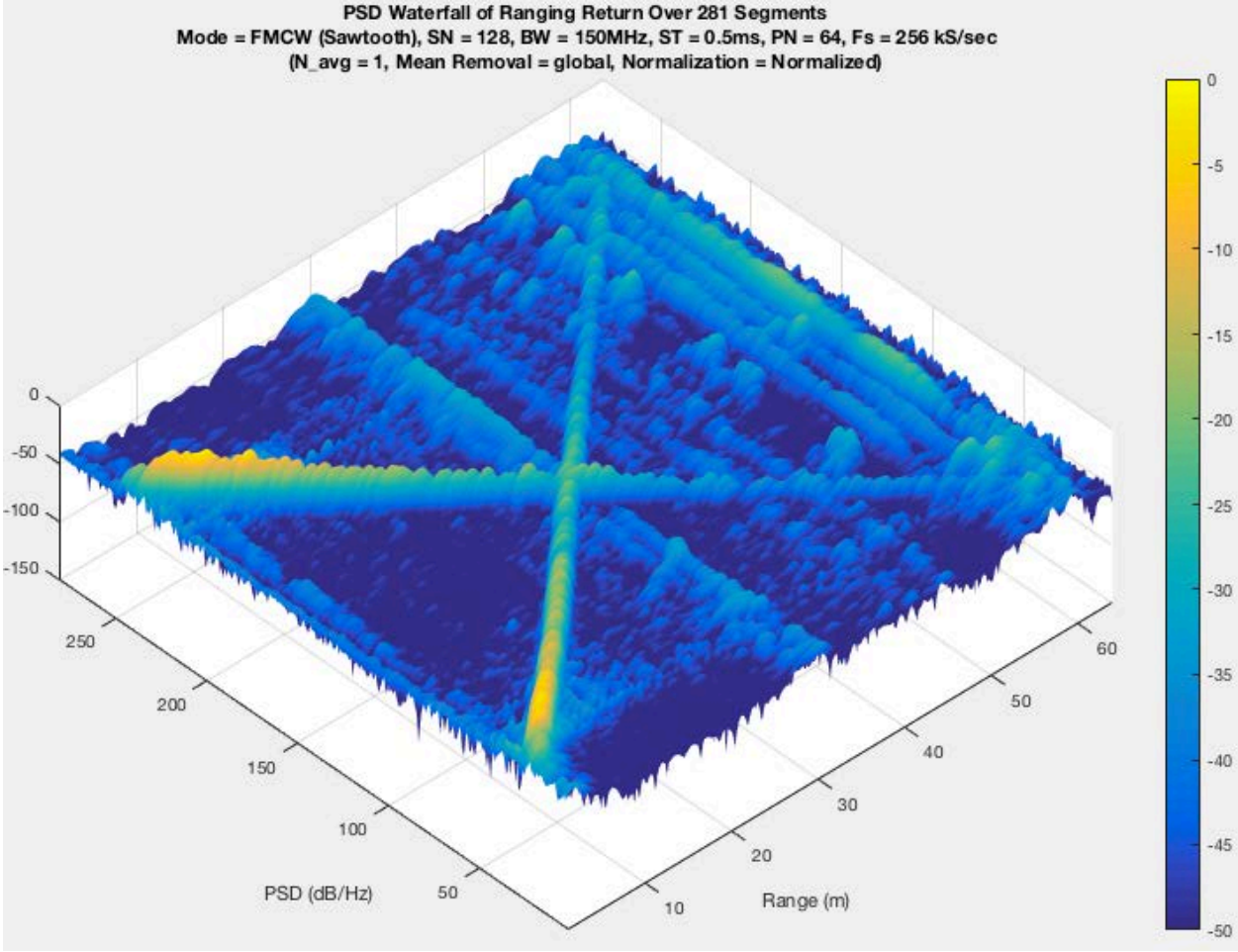

Figure 2.5 3D plot of a RADAR return waterfall plot showing the same data set as in Fig 2.4-ii.

Figure 2.6 Parking Lot test setup with RADAR facing down straight parking lot section

Figure 2.7 RADAR Reflector test used in pedestrian test scenarios

For validation of this approach we then took our setup to a Union Pacific railyard and conducted tests observing trains entering and exiting the railyard as well as railyard workers walking across the yard.

The purpose of this radar field test was to collect additional data for specific scenarios involving trains, locomotives, and their railcars, and to capture this information by radar to learn from and study the signals registered and viewed from the radar's perspective. The analysis of this data was useful to improve and/or add features to the real-time Software-Defined Object Tracking algorithm called **SDROT1** to be employed as a safety mechanism in a rail yard environment. The site at the Council Bluffs area and the configuration employed is illustrated below:

Figure 2.8 Slight side-view of the Rails West/Council Bluffs site radar configuration, showing radar placement, and main train path. There is a grade crossing at the intersection of 16th Ave. and S. Main St.

This site was chosen due to the proximity to the Rails West museum, pictured to the left of Fig. 2.8 above, which has a series of adjacent parallel tracks. Not shown, and south-east of these tracks is the Union Pacific Railyard in Council Bluffs. We were located on North-East corner near cross-streets o f *16th Ave*. and *South Main St*. This placed us in near proximity to the nearest track to us, and oriented the radar either SOUTH across 16th Ave, or WEST across South Main St.

depending on whether the train was arriving or departing from the aforementioned Rail Yard. If the train was arriving (taking on a South-East direction), then the radar was oriented WEST, but if the train was departing (taking on a North-West direction), then the radar was oriented SOUTH. As can be seen from Fig. 2.8 above, the distance to the track position was approximately 20m (meters) regardless of the two orientations used.

Figure 2.9 below shows a top view of the site chosen along with some important rough measurements of various points of interest, including the distances from the radar's position to the nearest rail track points, as well as distances to traffic lanes at various points, since we were also able to collect data on ongoing traffic while trains were not present.

Figure 2.9 Rails West/Council Bluffs Field Test Configuration (Top View). The red shaded area shows the main area of focus. The Iowa Interstate Railroad Council Bluffs Yard is South-East of the above traffic intersection along the Train Path indicated in the above figure.

We made use of Ancortek's SDR580B-KIT radar set, shown in Fig. 2.10. This is a 5.8 GHz radar, with an operating bandwidth of 100, 150, 300, and 400MHz. However, all of the data collected was done at a fixed bandwidth of 150MHz. The maximum effective range is spec'd by Ancortek at < 103m, and it can operate in Frequency-Modulated Continuous Wave (FMCW)

mode (Sawtooth and Triangular), Frequency-Shift Keying (FSK), and Continuous Wave (CW) modes. However, all of our data was collected specifically using FMCW (Sawtooth) mode.

SDR Evaluation Kit	SDR KIT 580B
Waveforms	FMCW/FSK/CW
Frequency Range	5.6 — 6.0 GHz
Expandable Frequency Range	5.2 — 6.0 GHz
Antenna Beam Range — Horizontal / Vertical	Patched Antenna 40°/20°
Bandwidth	100/150/300/400 MHz
Expandable Bandwidth	800 MHz
Power Output	19 dBm
Noise Figures	3.4 dB
Effective Range at RCS 1sm, Gain 15 dBi, SNR 0 dB	< 103 m

Figure 2.10 Ancortek's SDR 580B-Kit used in all tests conducted.

The radar is controlled via USB where it is operated from a laptop via a custom-written software, called **gSDR**, which runs in MATLAB. This software was written for efficient data collection in a variety of modes, and additional control parameters beyond what is provided natively by the software provided by Ancortek. It also allows us to do very long recordings of data over long periods of time, and record data efficiently to disk, but it also allows us to immediately re-load and playback this data for examination, which is not possible with Ancortek's software at the present time. A screenshot of **gSDR**is seen below.

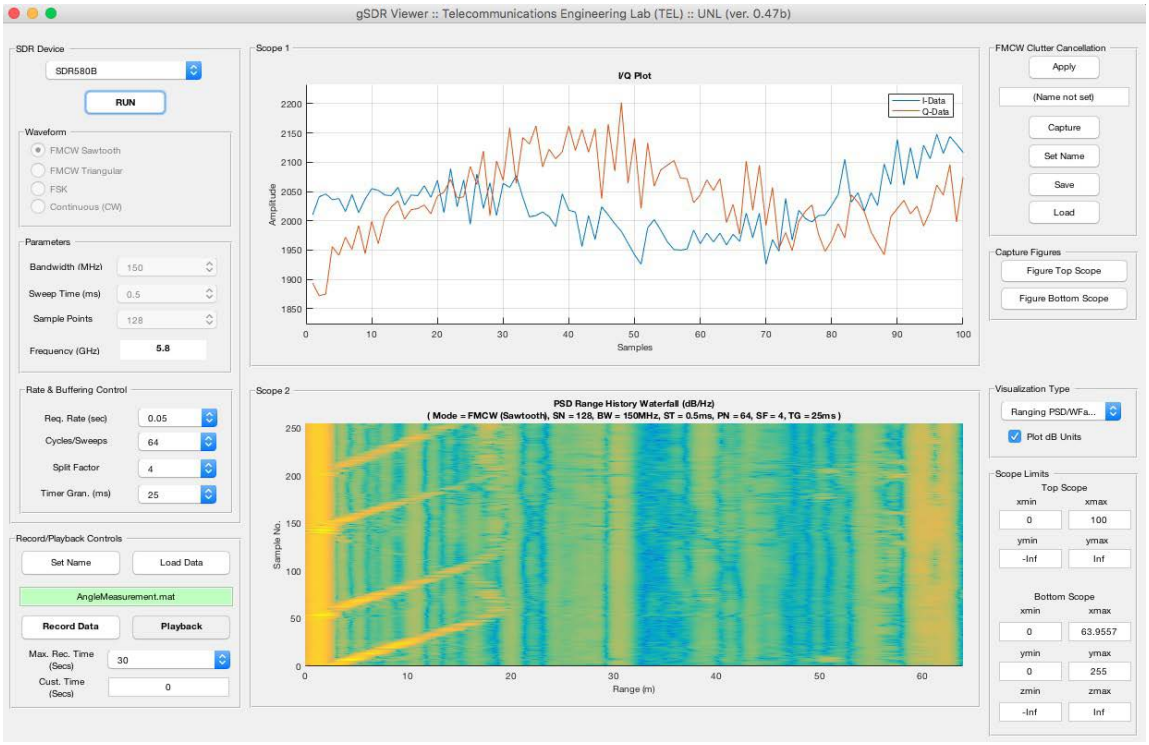

Figure 2.11 gSDRsoftware, custom-written software by UNL's TEL group, running in MATLAB.

Physically, the radar was mounted on a tripod at approximately 10ft from the ground. This tripod was then stabilized by an adjacent pole to minimize flexing, and pointed in the

directions previously discussed. Example photos taken of the experimental setup are illustrated below.

Figure 2.12 (left) Radar setup with laptop, tripod and video camera.
(right) Closeup of radar transmit and receive antenna and control unit (blue box).

Along with the radar, and tripod, we had a laptop mount with a sunshade to allow us to see the screen more easily, and a video camera was also mounted on a tripod to obtain visual record of the radar tests. A portable battery source was used to power both the radar as well as the laptop. A heavier battery was used to maintain the large radar tripod from tipping over due to wind effects.

Figure 2.13 Another view of the passing train.

Figure 2.14 Radar Field testing setup while a locomotive passes by. Most of the time was spent waiting for trains. Here the train is departing from the Railroad Council Bluffs Yard with the train heading North-West, while the radar is pointed SOUTH across *S. Main St*.

Chapter 3 Field Tests

3.1 Field Test: Settings and their Descriptions in gSDR

In this section, more information is given about each test. Screenshots of some of the visualization data acquired (mostly *waterfall* plots of Power Spectral Densities or PSD) are also presented for reference. Before going over those tests, let's briefly discuss the settings employed and also help convey their meaning.

All tests were conducted with the following settings:

- Mode: FMCW (Sawtooth)
- Sweep Time (ST) = 0.5ms
- Bandwidth (BW) = 150MHz
- Sample Number (SN) [aka. Samples per Sweep] = 128
- Cycles/Period Number (PN) [aka. Sweeps per Frame] = 64
- Split Factor = 4
- Timer Granularity = 25ms
- Req. Rate (frame rate) = 0.1 sec (10 Hz)

An overview of some of these parameters are discussed below:

T h e ***sweep time*** (ST) determines the time for one single sweep, with the modulating waveform changing the base frequency (5.8 GHz) by the *bandwidth* BW (of 150MHz). This bandwidth was chosen because it provided the appropriate detection range of approximately 60m. This matched the dimensions of the field test area in terms of depth (or length) as illustrated in Figures above.

A total of 64 **cycles** (PN) are collected and stored in the buffer for I/Q data for each data acquisition period, which we refer to as an *acquisition segment* or simply '**segment**' (sometimes called a 'frame'). In turn, a dataset (as stored on disk) contains many such segments, each 64

cycles in length, which is determined by the *request rate period* set in the UI panel of **gSDR**. For example, if the request period is 0.1sec (which translates to requesting 10 segments/second), then a 30 sec recording session will store at most 300 segments, each containing 64 cycles. Loosely speaking, this gets stored as a 300x64 matrix. Each 'cycle' or 'sweep' contains **SN points**, which in our case was 128 points or data samples, so a segment of 64 cycles would contain 64x128, or 8192 samples, one for the *I* data and one for *Q* data.

The ***split factor***, in turn, determines how a single segment (consisting of these 64 cycles) are split up into 'burst-read' groups from the radar before the segment buffer is considered 'full'. For example, a split factor of 4 means that the 64 cycles were read from the radar's hardware in burst-groups of four, each containing 16 cycles. The *timer granularity* (TG) determines how quickly the radar attempts to get its burst-read cycle data between groups. For example, 16 cycles were read in a burst as fast as possible by the hardware, then 25ms elapsed before the following 16 cycles burst-group was requested from the hardware and obtained, etc., until a complete single segment (of 64 cycles) was fully acquired.

In summary, each of these settings control the accuracy and the sensitivity of the radar in accordance to features and limitations of both the hardware, and provided hardware drivers by Ancortek, but work against the responsiveness as well as 'frame rate' of the radar's software, so an appropriate balance must be chosen between all these settings. Changing one attribute or setting to obtain a gain in some respect sacrifices some other attribute as a result.

Since this document presents a summary of what was collected, and images that follow only show a single snapshot at a moment in time of each data test performed, no doubt one may want to replay this data yourself so that can see the results in action. This can be done directly using MATLAB's **gSDR**(our custom app) by loading the data and engaging the PLAYBACK mode

when you hit the **RUN** button. It should be noted that the data presented here may have been 'decluttered' to remove some of the clutter present and you might not get exactly the same images as are shown in the pages that follow. In any case, to replay the datasets yourself perform the following steps in MATLAB (provided you've installed the **gSDR**toolbox):

- If you have the SD-radar hardware attached via USB, start **gSDR** by typing **gSDR** and then pressing [Enter]. If you do NOT have hardware attached (i.e., the radar itself), you should start **gSDR** by entering **gSDR('WITHOUT_HW_DEPENDENCIES',true)**, and then hitting [Enter].
- When the UI appears, under 'SDR Device' drop-down menu, select the device (even if you do not have hardware attached). For us, select **SDR580B** from the drop-down menu.
- At the bottom-left corner under 'Record/Playback Controls' click on the **[Load Data]** button, and find the ***.mat** file containing the data in your computer, directory, or disk. For example **rw00_TrainApproaching.mat**. Do NOT select filenames with trailing numbers, such as "**rw00_TrainApproaching-001.mat**" as this is just the data associated with the main file.
- Engage PLAYBACK by hitting the **[Playback]** button. This will turn the filename text box as green, to let you know that PLAYBACK mode is engaged.
- Under 'Rate & Buffering Control', change the '**Req. Rate (sec)**' value from the drop-down menu. This will control how fast the data is played back. The fastest playback can be achieved by selecting **0.05**.
- Select the 'Visualization Type'. This control is to the right of the bottom scope. You might want to start with '**Ranging PSD/WFall Plot**' to see waterfall plots. Also

select whether you want the scope data to be visualized logarithmically or not by clicking on '**Plot dB Units**'. Select other visualization types if you'd like to see data in different visualization modes. The visualization mode cannot be changed while the simulation is running. If you want to change the settings you need to STOP the simulation, then change the visualization mode, and then re-start it (from the beginning).

- Hit the **[RUN]** button to start PLAYBACK. When the data is exhausted, it will automatically stop.
- Reload new data (by going back to step (3)) or repeat the playback as many times as you want (by going back to step (7)).

This is only a brief summary of the steps. A supplemental video was also created to briefly demonstrate these steps. In addition, the video discusses how the data can be decluttered for datasets that either already include a **Clutter** dataset associated with it (often saved as **Clutter.mat**), and, for cases where no clutter dataset was collected, it also shows you how to create and declutter the dataset, at least minimally.

3.2 Field Tests at Union Pacific Railyard

Field Tests were conducted at the Union Pacific Council Bluffs railyard. This is just North-West of the Council Bluffs in Iowa. A total of six field tests were performed, which are summarized below. A test number (ranging from 1-6) is assigned to each field test along with a name that closely matches the name given in MATLAB (on disk) and a brief description. A detailed set of descriptions for each test will then follow.

3.2.1 Field Test List & Brief Summary

- "**Test00_TrafficOnly**" – Data consisting of traffic only.

- "**Test01_TrafficOnly**" – More data consisting of traffic only.
- "**Test02_TrainApproaching**" – Data of an arriving locomotive, heading SOUTH-EAST, towards the Iowa Interstate Railroad Council Bluffs Yard. This was the longest train captured.
- "**Test03_TrainDeparting**" – Data of a departing locomotive, heading NORTH-WEST from the Iowa Interstate Railroad Council Bluffs Yard. Train stopped at the grade crossing between 30-to-60secs, then continued on.
- "**Test04_TrainApproaching**" – Data of an arriving locomotive, heading SOUTH-EAST, towards the Iowa Interstate Railroad Council Bluffs Yard. Due to technical issues data was captured beginning at the moment the train had already reached the grade crossing.
- "**Test05_ClutterForTest04**" – This was a very short segment of clutter data that can possibly be used for **Test04**to perform clutter cancellation. It is mostly for internal use only. It will not be discussed any further.

Notes:

- **SNR** stands for Signal-to-Noise Ratio.
- **RCS** stands for *Radar Cross-Section*.
- **FOV** stands for *Field-of-View*.

Test00 – Traffic Only

Figure 3.1 Field Test configuration for Test 00.

For this test, the radar was pointed SOUTH, across *16th Ave*, while ordinary East-bound and West- bound traffic was observed. Unlike previous field tests we've performed, whereby small sedan-type vehicles had been used, this gave us the opportunity to collect data for a variety of vehicle types and sizes: from sedans, pickup trucks, flat-bed trucks, large cement trucks with their rotating drums, as well as semi (freight) trucks which are considerably large, and posses a large RCS (radar cross-section). A snapshot of the waterfall plot is illustrated in the following figure.

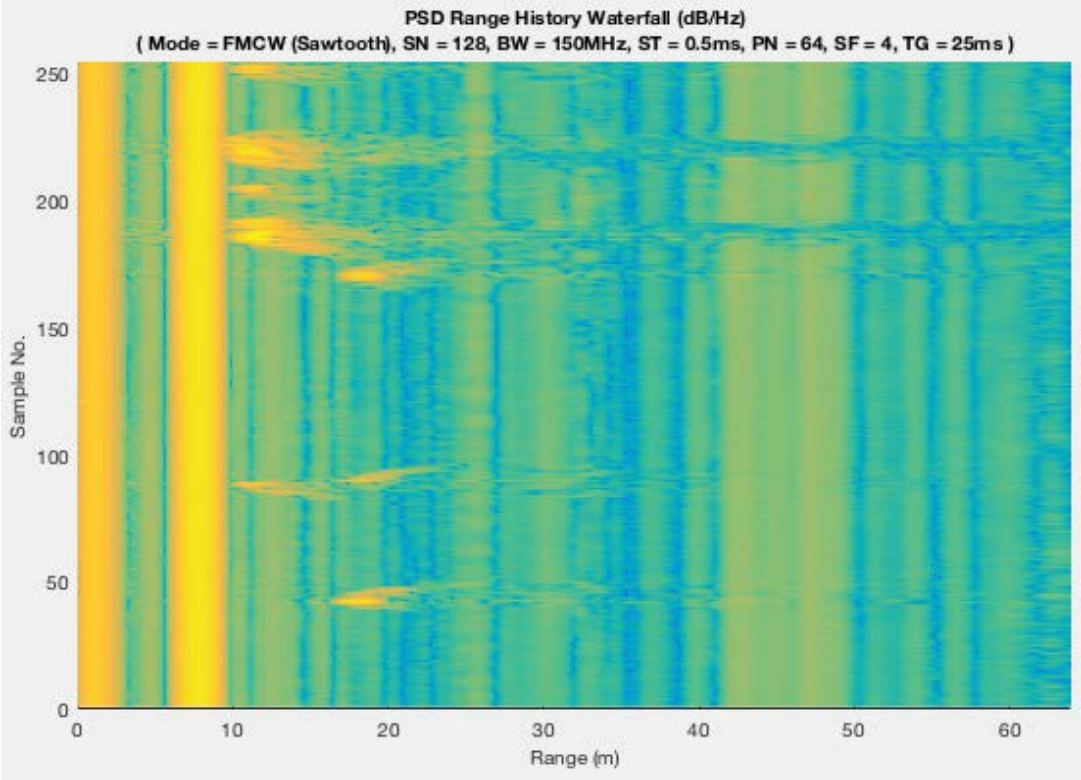

Figure 3.2 Waterfall plot of Power Spectral Density (PSD) for **Test00**.

It can be clearly seen from the above waterfall plot that the overall spectral [horizontal] *spread* observed is proportional to the vehicle size. Small vehicles register a small spread in the signal, while larger vehicles have a very large signal spread for all objects captured in a range less than 20m. However the signal spread itself occupies almost nearly the entire PSD range spectrum for large (semi trucks) vehicles.

It should be noted that for this, and all other subsequent tests, there is an offset error in the range values provided, which can be easily compensated for. From the radar's position we measured between 8.5m and 15.5m for the two traffic lanes in question. This is what is shown in Fig. 3.2. We can clearly see objects that are closer to 8.5-to-9m (obscured by the persistent vertical trace from a stationary object), and the traffic in the opposite lane at around 15m or so. The rest is the signal spread from each of these objects—again depending on object class size.

3.2.1.1 Test01 – Traffic Only

The configuration and test outcome for **Test01**is exactly the same as that for **Test00**. Again, the purpose was to capture a 2nd recording between 30 to 60secs of traffic-only data. Once again, vehicles of a variety of size classes were captured. The radar was still pointed in the same direction: SOUTH, across *16th Ave*. The sample snapshot of the waterfall plot for this particular dataset shows some very large signal spreads than captured in **Test00**. As can be seen from the following waterfall plot, a greater variety of *larger* vehicles were captured during this test. Again, to remind the reader, this is traffic only. NO locomotives or trains were captured during this particular recording period.

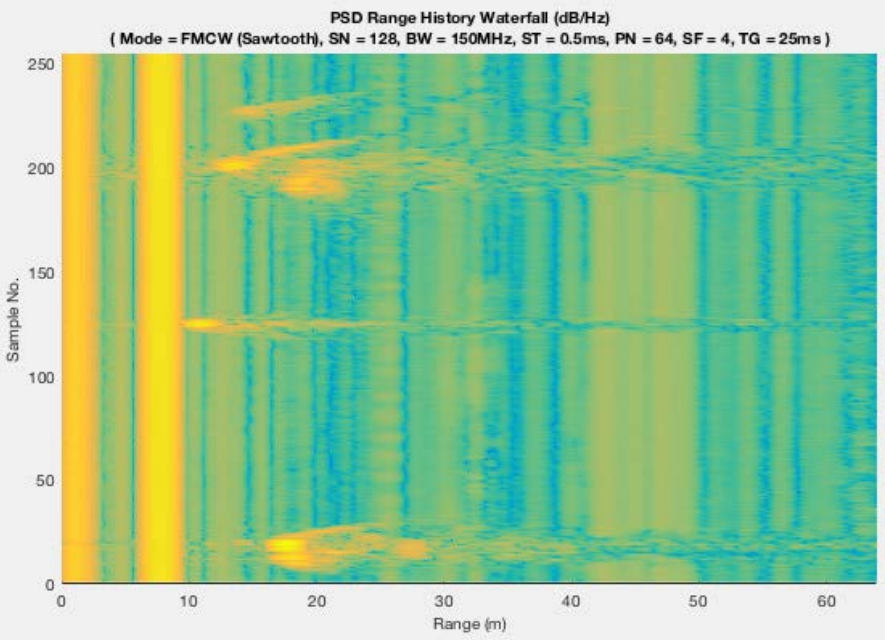

Figure 3.3 Waterfall plot of Power Spectral Density (PSD) for **Test01**.

These particular horizontal signal spreads were due to large vehicles doing a right-turn directly in front of the radar, which is why their radar returns are 'thicker' (vertically) in addition to exhibiting a wide signal 'spread' across a very wide spectrum, as already discussed. Such phenomena are easy to see at such close proximity.

3.2.1.2 Test02 – Train Approaching

The configuration for this test is shown in Fig. 18. In this particular test we captured the arrival of a train (locomotive and corresponding rail cars) at the *Iowa Interstate Railroad Council Bluffs Yard*, at a slow speed (<10mph) heading SOUTH-EAST. The radar was pointed WEST, so that it somewhat faces the train and its locomotive.

Fig. 3.5 shows a snapshot of the Power Spectral Density (PSD) waterfall captured by the radar. It shows something that we theorized and expected: the train (and all corresponding rail cars) present such a large radar cross-section (RCS) that, given the proximity of the radar to the train, it generated a very large signal spread, laying out 'traces' in the waterfall plot that move together as a group. This is in great contrast with the PSD of a pedestrian or vehicle, which manifests itself as a very localized *peak* in the waterfall plot. Notice this is NOT the case at all for an approaching train. To put it bluntly, the signal trace is 'all over the place' here, which we expected.

Another peculiar behavior observed in the waterfall plot of Fig. 3.5 is that the first few traces of the train in the waterfall plot are *stronger* than the others. This shows how object geometry plays an important role in how the radar sees them. In this particular instance the first few railcars were locomotives, with sharp edges, providing a stronger radar return, while the remaining railcars for the remainder of the recording period mostly cylindrically-shaped, generating a slightly softer radar return.

Figure 3.4 Field Test Configuration for **Test02**.

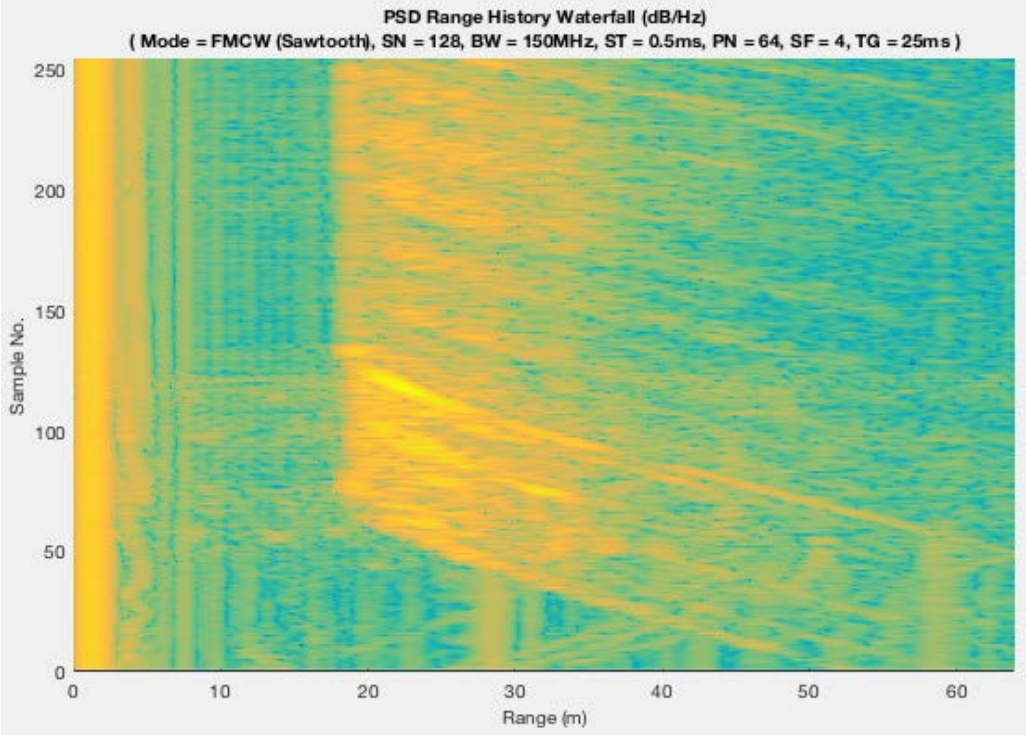

Figure 3.5 Waterfall plot of Power Spectral Density (PSD) for **Test02**. Notice return is initially strong, but then generally softer.

Figure 3.6 Initial set of locomotives, with sharp edges and rectangular nature provides a larger RCS to the radar.

Figure 3.7 The remaining locomotives were more cylindrical causing the radar signals to spread out and yielding a 'softer' return.

3.2.1.3 Test03 – Train Departing

Figure 3.8 Field Test Configuration for **Test03**. Note the 'Train Path' is actually opposite of what is shown above.

In this test, we collected data for a train that was departing from the *Iowa Interstate Railroad Council Bluffs Yard* as shown in the above figure. Since the train was departing, it was heading opposite than is indicated by the “Train Path” in Fig. 3.8. That is, the train was heading NORTH-WEST, while the radar was oriented SOUTH, across *16^{t} Ave* as shown.

Fig. 3.9 shows the Power Spectral Density (PSD) waterfall plot of the train when it was first detected by the radar. Once again, we observed a very large signal return consisting of many signal 'traces' in the waterfall plot. During the recording of this particular test, the train's locomotive came to a full stop at the grade crossing for about 30 seconds. This momentary 'stasis' by the train was captured towards the end of Fig. 3.9. After 30 seconds or so, the train began moving again and continued in the same direction until it cleared the grade crossing.

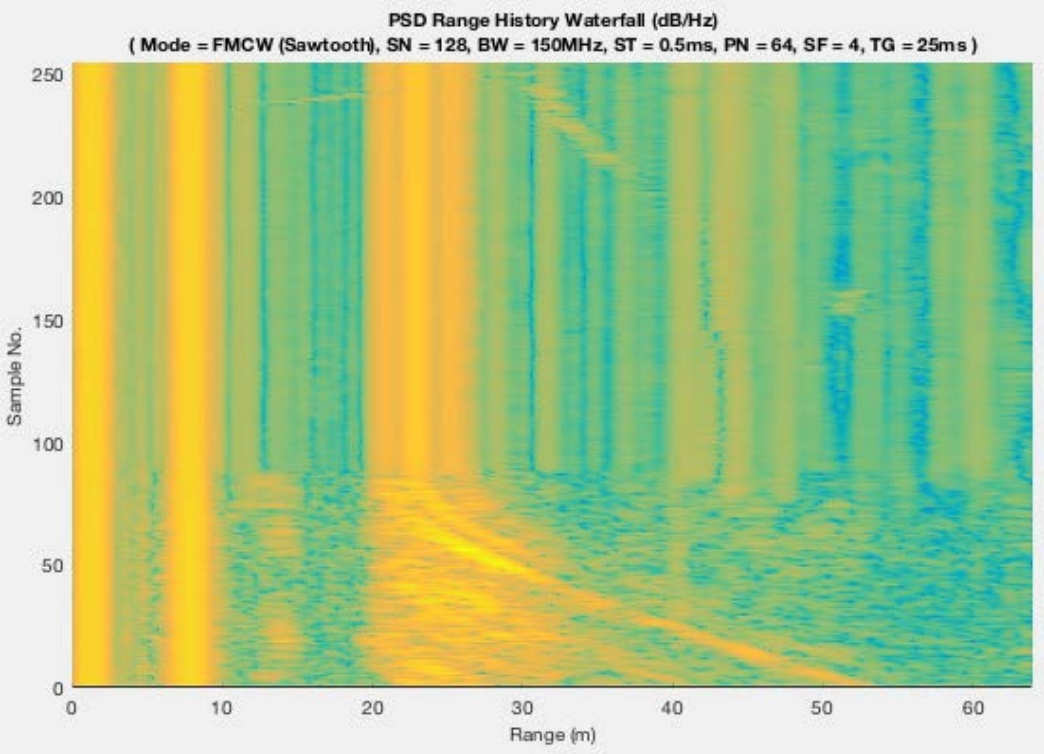

Figure 3.9 Waterfall plot of Power Spectral Density (PSD) for **Test03**as it entered the radar's FOV.

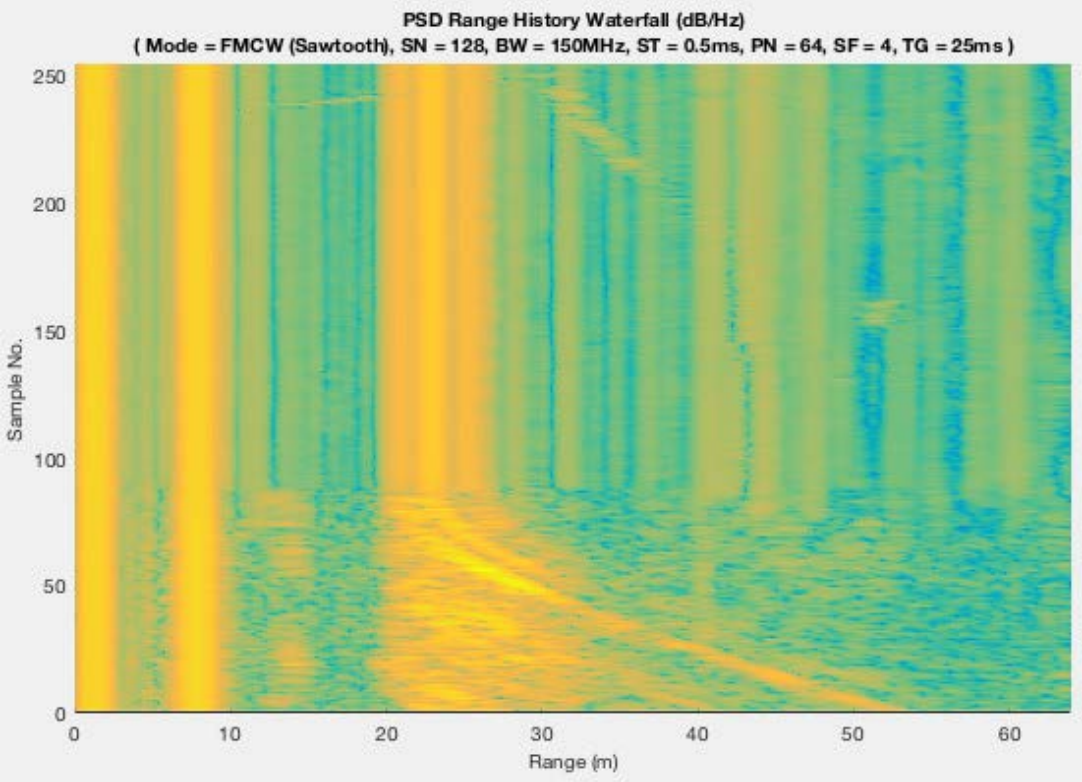

Figure 3.10 Waterfall plot of Power Spectral Density (PSD) for **Test03**. It also shows a period of time while the locomotive remained stationary (temporarily stopped) before continuing on, showing a very large spread between 20-to-27m or so.

3.2.1.4 Test04 – Train Approaching

Figure 3.11 Field Test Configuration for **Test04**.

This test consisted of another train approaching along the train path, heading SOUTH-EAST towards the Iowa Interstate Council Bluffs Rail Yard. The radar was pointed WEST, across *South Main St.*

For this particular test we had a bit of technical difficulties getting the radar system to start recording. This was due to the USB cable detaching while the radar was reoriented for the oncoming train. As a result, data was captured from the point the train had already arrived at the grade crossing as shown in Fig. 3.11. Furthermore, the train was very short, containing no railcars except a multiple locomotive consist of about 3-5 cars. It was a short recording. After the train cleared the radar, we captured some more ordinary vehicles passing by.

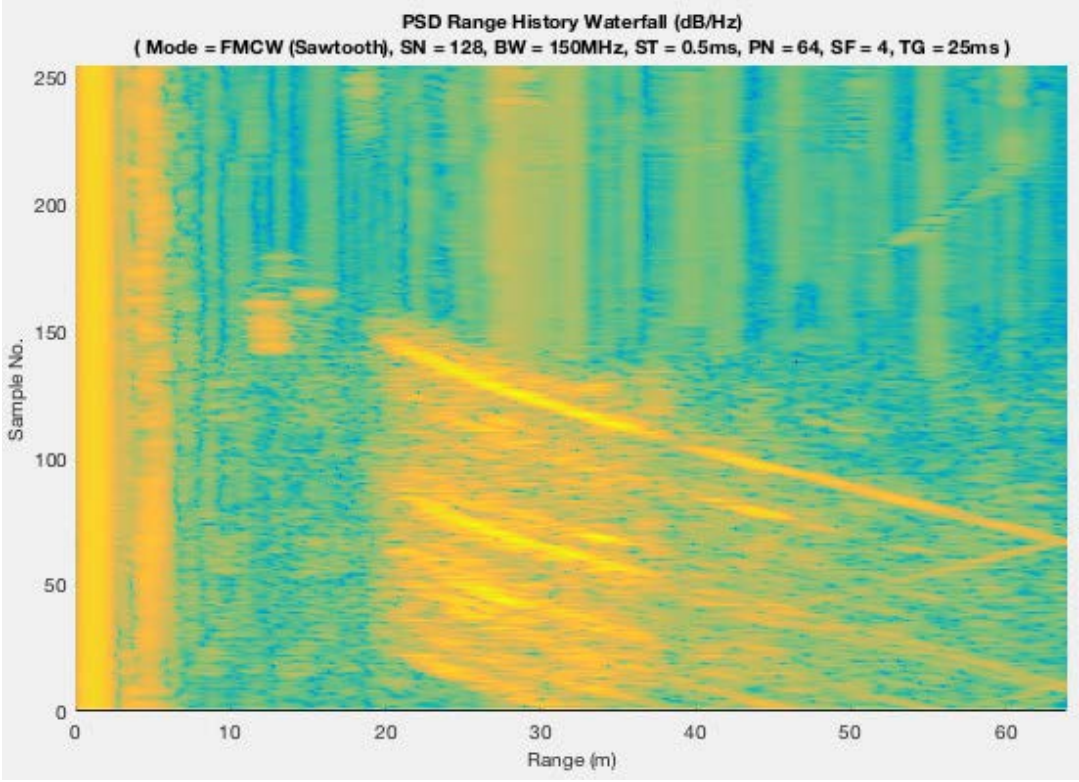

Figure 3.12 Waterfall plot of Power Spectral Density (PSD) for **Test04**.

The primary goal for collecting train data for this third round of field test was to verify a theory surrounding the question of '*what would the radar see?*'. It was theorized that instead of observing a single localized peak as we have seen for small objects, that a train would provide such a large radar cross section (at cross proximity) to the radar that it would register as a signal with many peaks exhibiting large signal 'spread', making it difficult to ascertain the true position of the object. This is precisely what was observed in some of the waterfall plots shown earlier for those cases where a train was captured. The below figure is also another example of a single snapshot obtained from the waterfall plot (a single 'slice' if you will). As can be seen there are several peaks corresponding to various 'radar reflective' parts of the train, but it is difficult to ascertain (at least from this data alone) where the train's position truly is, or whether this is one object, or 4 objects.

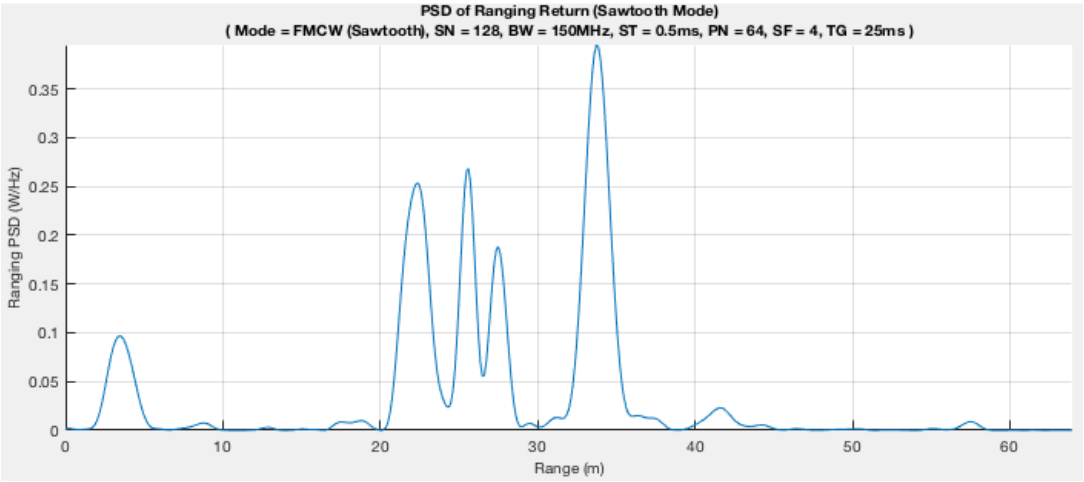

Figure 3.13 Power Spectral Density (PSD) of a single 'slice' of the waterfall plot for **Test02**.

This demonstrates some of the challenges that will have to be tackled by our real-time object-tracking algorithm called **SDROT1**, and we expect to be a great source of difficulty. Typically **SDROT1**will look at individual *peaks* from localized objects, and can maintain a pretty good 'lock' so long as this peak is considered to be 'persistent', as viewed by the radar. This is straight-forward for small localized objects such as vehicles and pedestrians. The situation, however, becomes more challenging when there isn't a singular isolated peak that can be mapped to each individual object. However, in the case of the train signal, the spread is so great, and the reflections non-localized that it will be difficult to determine what is a unique object, and/or whether new appearing peaks are still related to that of a train from **SDROT1**'s perspective.

It may be the case that at this point, relying entirely in solving the object-tracking problem purely from a signal-processing approach won't be sufficient enough, and a such, stochastic, and machine learning methods will have to apply in order handle the large level of uncertainty that

comes with the radar signal from a large train and locomotive consist as was shown in the train-related waterfall plots.

Presently, however, this is only speculation. The *next step* at this juncture is to start analyzing the data from a signal-processing approach and look at this signal from a variety of perspectives (such as the joint range-doppler maps) as well as behaviors in signal spread to determine if these features, when used jointly, can help us tackle radar signals when they are reflected from a train and/or locomotive.

The following figure summarizes our signal processing approach, currently implemented by our tools and successfully validated in multiple field tests.

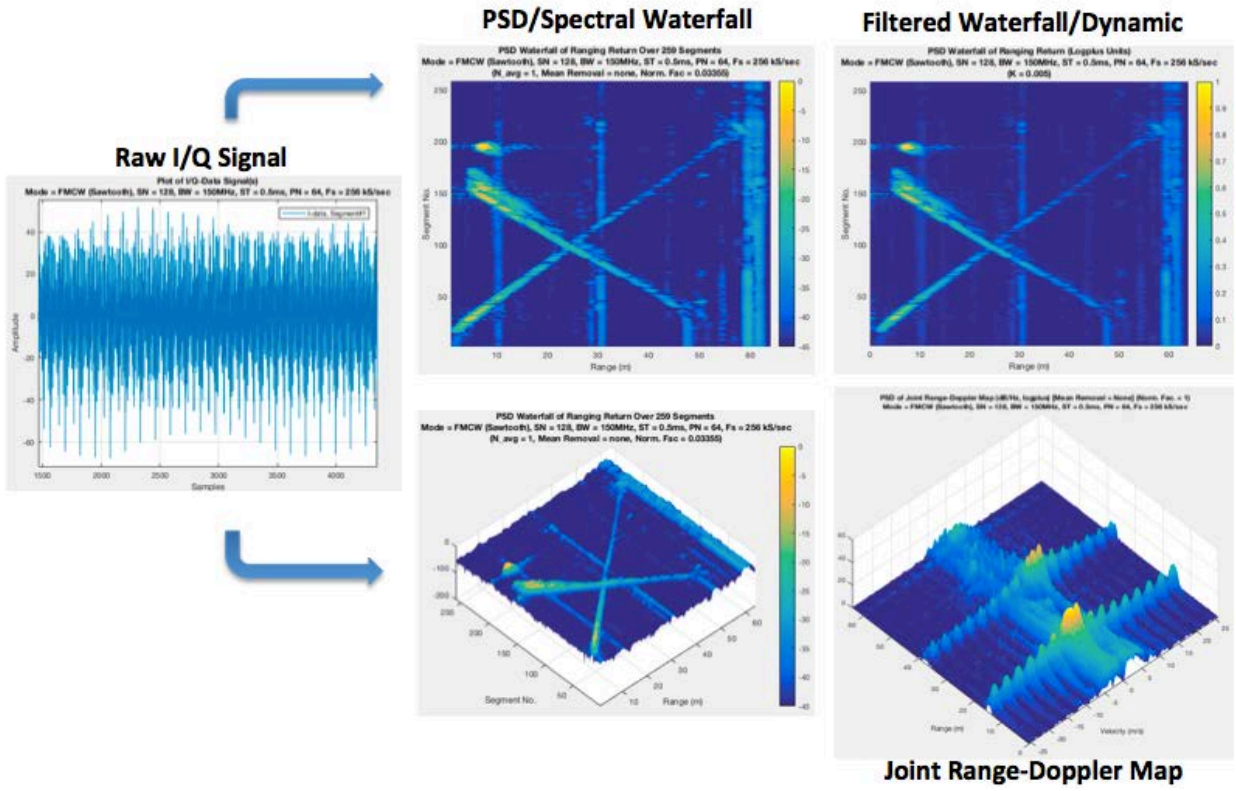

Figure 3.14 Signal Processing Phases in our SDROT tool (Software Defined RADAR Object Tracking)

Finally, below is a figure illustrating the object tracker itself in action, in which the tracker annotates the traces observed due to objects within the field of view of the RADAR and attributes them intelligently to identified objects managed over time. This also provides the basis of the object classification we made forays into researching.

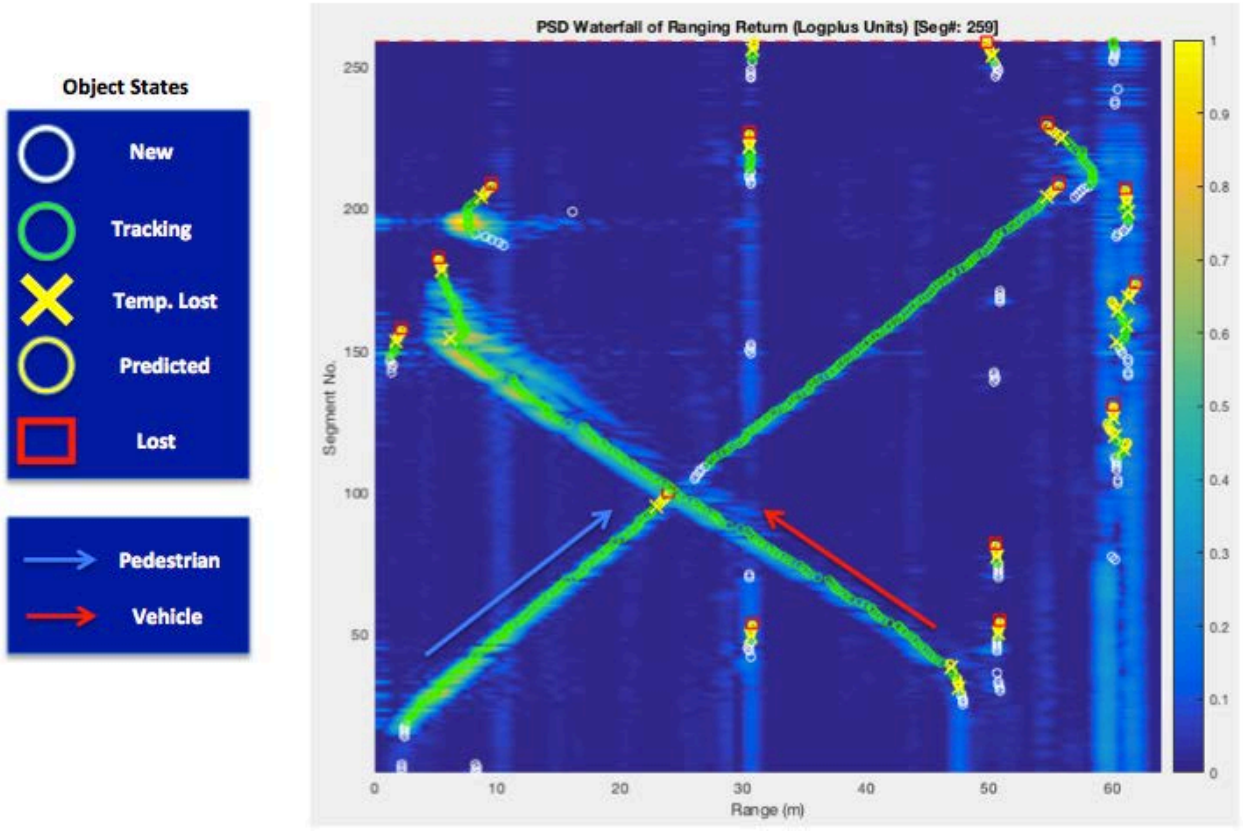

Figure 3.15 Object Tracking over Time

We'll be able to better understand what sort of challenges we can immediately tackle and solve to continue moving **SDROT1**, our real-time object- tracking algorithm forward.

Chapter 4 Summary and Conclusions

4.1 Summary

This report provided a brief summary surrounding the *third* round of field tests whereby data was collected using Ancotek's Software-Defined Radar (SDR) technology. This third round of tests focused on collecting data of approaching and departing trains, by setting up at the Rails West Museum site, near the Iowa Interstate Railroad Council Bluffs Yard, in Council Bluffs, Iowa. The report discussed the configuration setups for collecting this data, listed the tests that were conducted for collecting data, and provided a slightly more detailed summary of each dataset that was collected along with a snapshot of the waterfall plots composed of the Power Spectral Density obtained by the radar.

To summarize, these round of field tests focused on helping to answer the question that the research team had theorized regarding the behavior of the radar signals that would be collected from a passing train. It was theorized that instead of a small localized peak associated with an object in question, we would instead get large signal traces, with large spread and reflectivity, and this is precisely what we obtained.

The data shows that train detection, train tracking is possible as the signal of the radar return is localized. However, a great deal of signal analysis will have to take place for us to better understand how to modify our real-time object-tracking algorithm (**SDROT1**) to tackle the presence of such large objects with other small items in a close proximity.

4.2 Publications Resulting from Research

During this project we have thus far published three conference paper, and are in the process of completing the writing on two more papers. The first published conference paper is titled “A Review of Workspace Challenges and Wearable Solutions in Railroads and

Construction", by S. Banerjee, M. Hempel, and H. Sharif, presented at and published in the conference proceedings of the 2017 International Wireless Communications and Mobile Computing Conference (IWCMC). The second paper was published at the 2017 ASME Joint Rail Conference (JRC). It is titled "A Survey of Railroad Worker Protection Approaches and System Design Considerations", written by S. Banerjee, M. Hempel, and H. Sharif. The third paper is titled "A new Railyard Safety Approach for Detection and Tracking of Personnel and Dynamic Objects using Software-Defined RADAR", by S. Banerjee, J. Santos, M. Hempel, and H. Sharif, and was presented and published at the 2018 ASME Joint Rail Conference (JRC).

4.3 Conclusions and Future Work

Railyards are a dangerous workplace, and being able to contribute to improving the safety of railyard workers is a truly appreciated opportunity for our team. We leveraged our expertise in multi-sensory data acquisition and developed a system for object detection, localization, and classification. Once these parameters are known a threat index to a railyard worker's safety can be computed and alerts can be sent to the railyard worker and colleagues in the vicinity. This contributes to increased situational awareness and faster responses in case of an incident. We have shown that the combined use of vision-based systems and RADAR achieves robust results and has great potential to be developed further into a full-fledged solution. Combined with wearable systems used as personal health monitors and for alerting, this solution can greatly contribute to improving the safety of railyard workers. For future work we would like to continue the exploration of this system, research the wireless communication and wearables aspect, as well as explore ancillary uses of this technology, such as for trespasser detection. There is tremendous potential in this technology and we look forward to further exploring its many

applications. We would like to thank the Union Pacific Railroad for all their assistance with this project.

References

1. S. Banerjee, M. Hempel, and H. Sharif, “A Review of Workspace Challenges and Wearable Solutions in Railroads and Construction”, 2017 International Wireless Communications and Mobile Computing Conference (IWCMC).

2. S. Banerjee, M. Hempel, and H. Sharif, “A Survey of Railroad Worker Protection Approaches and System Design Considerations”, 2017 ASME Joint Rail Conference (JRC).

3. S. Banerjee, J. Santos, M. Hempel, and H. Sharif, “A new Railyard Safety Approach for Detection and Tracking of Personnel and Dynamic Objects using Software-Defined RADAR”, 2018 ASME Joint Rail Conference (JRC).